Bisection Algorithm based Indirect Finite Control Set Model Predictive Control for Modular Multilevel Converters

Saad Hamayoon[1], Morten Hovd[1] and Jon Are Suul[1,2]
[1]*Department of Engineering Cybernetics, Norwegian University of Science and Technology, Trondheim, Norway*
[2]*SINTEF Energy Research, Trondheim, Norway*
email:saad.hamayoon@ntnu.no

***Abstract*—In this work, an idea based on the bisection algorithm is used to reduce the computational burden of indirect finite control set model predictive control (FCS-MPC) for modular multilevel converters (MMCs). The proposed method greatly reduces the search space for reaching the optimal insertion index (number of submodules to be inserted). Therefore, the strategy proposed offers similar steady-state and dynamic performance compared to full indirect FCS-MPC at a much lower computational burden. A new cost function is also proposed for indirect FCS-MPC which eliminates the need for an outer loop or additional control of differential current to regulate the summation voltages in each arm. The results of the proposed strategy are validated through simulations in MATLAB/Simulink.**

***Index Terms*—circulating current control, model predictive control, modular multilevel converter (MMC), capacitor voltage balancing**

I. Introduction

In recent years, modular multilevel converters (MMCs) have been adopted by the industry due to their excellent features such as high efficiency, redundancy, low harmonic content and modular nature [1]. Due to these features MMCs are now becoming the dominant technology for high voltage direct current (HVDC) transmission systems. However, the multi input multi output (MIMO) nature together with the presence of internal dynamics makes the control problem of MMC difficult [2].

In the research literature, many control methods have been investigated for MMCs [3]–[5]. Among these, model predictive control (MPC) is an effective method to deal with MIMO and non-linear systems. Indeed, MPC can handle multivariable interactions and system constraints in a systematic way.

For power converters, finite control set model predictive control (FCS-MPC) is usually applied. FCS-MPC for MMCs can be broadly classified into three categories *i.e.* direct, indirect and reduced indirect FCS-MPC. In direct FCS-MPC, all the possible switching combinations are evaluated against a predefined cost function and the one that minimizes this cost function is then applied to the MMC. This method has the best performance at the cost of very high computational burden. The high computational burden is due to the very high number of switching combinations in MMC.

In order to deal with the problem of high computational requirements, the concept of indirect FCS-MPC [6] for MMCs has been developed. Instead of evaluating all switching combinations, this approach searches for the voltage level that minimizes the cost function. Thus, a separate sorting algorithm can be used for balancing the capacitor voltages. This significantly reduces the computational burden. However, the computational complexity is still too high for MMC applications with hundreds of SMs per arm. Therefore, many more research efforts were made resulting in reduced indirect FCS-MPC strategies [7]–[10]. These methods reduce the computational burden significantly by only considering neighboring voltage levels with respect to the previous sampling instant. However, the drawback of these approaches is that they suffer from slow dynamic response. The method in [11], proposed to distribute the SMs evenly into M groups with each containing X SMs. The overall computational burden was reduced to $2X+M+3$. However, no specific criterion is provided on how to group the SMs. A dual-stage MPC was presented in [12], utilizing voltage vectors redundancy in the first stage and redundancy of SMs in the second stage. This approach offers very good dynamic performance, however, its computational burden is much higher than the full indirect FCS-MPC strategy.

Recently, a modified reduced indirect FCS-MPC strategy was presented [13]. In this implementation, the number of SMs are allowed to change by more than one with respect to the previous sampling instant only in the initial timestep within the prediction horizon. This results in dynamic performance close to what is achieved with full indirect FCS-MPC. However, when dealing with large number of SMs per arm, the number of options to be evaluated in the initial time step need to be increased which increases the computational burden.

In this paper, a method based on the bisection algorithm is used to reduce the search for the optimal insertion index *i.e.* the number of SMs to be inserted in each arm. The idea can be considered as a special case of the branch and bound algorithm which is commonly used for the weighting factor selection in

978-1-6654-3635-9/21/$31.00 ©2021 IEEE

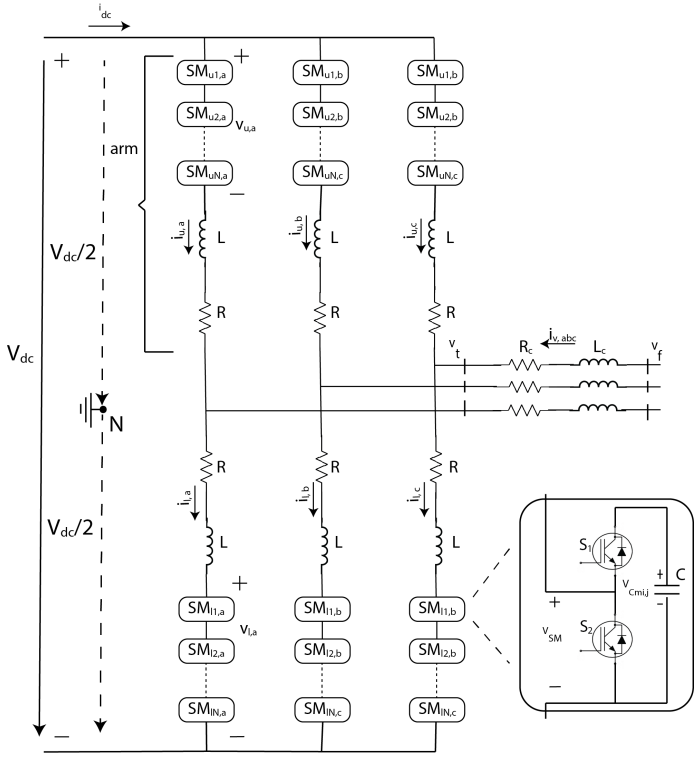

Fig. 1. Circuit Diagram of MMC

FCS-MPC [14]. The proposed method gives similar steady state and dynamic performance as the full indirect FCS-MPC at a much lower computational burden.

The remaining paper is organized as follows. The modeling and operation of the MMC is presented in Section II. The proposed control method along with new cost function is explained in Section III. The performance validation through simulation results is presented in Section IV.

II. Model of the MMC

The MMC topology used in this paper is shown in Fig. 1 and the modeling we apply for representing this topology is developed according to the approach explained in [6], [13]. The MMC consists of two identical arms *i.e.* an upper arm (u) and a lower arm (l) in each phase which are connected to the positive and negative dc terminal, respectively. The model of each arm includes N half-bridge submodules (SM), an inductor and a resistor. The arm resistance models the losses of the MMC and the arm inductor is used for limiting the harmonics and fault currents. The switching states of S_1 and S_2 determine the voltage level for each SM. The voltage level can be 0 or $v_{\mathrm{Cm_{i,j}}}$ where the index $m = u, l$ identifies the upper or lower arm, $i = 1, 2, \ldots, N$ identifies the individual sub-module within the arm, and $j = a, b, c$ identifies the phase. According to Kirchoff's voltage law, the mathematical model of the MMC shown in Fig 1 can be expressed as:

$$\frac{V_{dc}}{2} - v_{u,j} - Ri_{u,j} - L\frac{di_{v,j}}{dt} + R_c i_{v,j} + L_c\frac{di_{v,j}}{dt} - v_f = 0 \quad (1)$$

$$\frac{V_{dc}}{2} - v_{l,j} - Ri_{l,j} - L\frac{di_{l,j}}{dt} - R_c i_{v,j} - L_c\frac{di_{v,j}}{dt} + v_f = 0 \quad (2)$$

where $v_{u,j}$ and $v_{l,j}$ represent the upper and lower arm voltages of phase j, $i_{u,j}$ and $i_{l,j}$ represent the upper and lower arm currents of phase j, $i_{v,j}$ is the ac-side current, V_{dc} is the dc-side voltage, v_f is the grid side voltage, R is the arm resistance, L is the arm inductance, R_c and L_C are the equivalent grid side resistance and inductance, respectively.

The ac-side current, arm currents and differential currents are given by:

$$i_{v,j} = i_{l,j} - i_{u,j} \quad (3)$$

$$i_{u,j} = -\frac{i_{v,j}}{2} + \frac{i_{diffj}}{2} \quad (4)$$

$$i_{l,j} = \frac{i_{v,j}}{2} + \frac{i_{diffj}}{2} \quad (5)$$

where i_{diffj} is the differential current which flows through phase j of the MMC.

By subtracting (1) and (2) and using (3) the dynamic equation for ac-side current is obtained as:

$$\frac{di_{v,j}}{dt} = \frac{-(R+2R_c)}{L+2L_c} i_{v,j} + \frac{v_{u,j} - v_{l,j}}{L+2L_c} + \frac{2v_{f,j}}{L+2L_c} \quad (6)$$

Similarly, by adding (1) and (2) and using (4) and (5), the dynamic equation for the differential current is obtained as:

$$\frac{di_{diff,j}}{dt} = \frac{-R}{L} i_{diff,j} - \frac{1}{2L}(v_{u,j} + v_{l,j}) + \frac{1}{2L} V_{dc} \quad (7)$$

The arm voltages $v_{u,j}$ and $v_{l,j}$ depend on the number of SMs inserted in that arm. Assuming that SM capacitor voltages are well balanced at their reference values, the arm voltages can be expressed as:

$$v_{u,j} \approx \frac{n_{u,j}}{N} v^{\Sigma}_{u,j} \quad (8)$$

$$v_{l,j} \approx \frac{n_{l,j}}{N} v^{\Sigma}_{l,j} \quad (9)$$

where $n_{u,j}$ and $n_{l,j}$ are the number of SMs to be inserted in upper and lower arm respectively and $v^{\Sigma}_{u,j}$ and $v^{\Sigma}_{l,j}$ are the summation of all capacitor voltages in the upper and lower arm respectively.

The dynamics of the total arm capacitor voltages can be expressed as:

$$\frac{dv^{\Sigma}_{m,j}}{dt} = \frac{i_{m,j}}{C^e_{m,j}} = \frac{n_{m,j} i_{m,j}}{C} \quad (10)$$

where $C^e_{m,j}$ is the equivalent arm capacitance of the inserted SMs in arm m. Now equations (4) and (5) can be substituted into (10) to give the following dynamic equations for total arm capacitor voltages of both arms:

$$\frac{dv^{\Sigma}_{u,j}}{dt} = -\frac{n_{u,j} i_{v,j}}{2C} + \frac{n_{u,j} i_{diff,j}}{C} \quad (11a)$$

$$\frac{dv^{\Sigma}_{l,j}}{dt} = \frac{n_{l,j} i_{v,j}}{2C} + \frac{n_{l,j} i_{diff,j}}{C} \quad (11b)$$

Using the definition of $v_{u,j}$ and $v_{l,j}$ from (8) and (9) into (6) and (7) the dynamic equations for ac-side current and differential current are modified as:

$$\frac{di_{v,j}}{dt} = \frac{-(R+2R_c)}{L+2L_c} i_{v,j} + \frac{n_{u,j}v^{\Sigma}_{u,j} - n_{l,j}v^{\Sigma}_{l,j}}{N(L+2L_c)} + \frac{2v_{f,j}}{L+2L_c} \quad (12a)$$

$$\frac{di_{diff,j}}{dt} = \frac{-R}{L} i_{diff,j} - \frac{(n_{u,j}v^{\Sigma}_{u,j} + n_{l,j}v^{\Sigma}_{l,j})}{2NL} + \frac{V_{dc}}{2L} \quad (12b)$$

Using (11) and (12) the state space equation for one phase/leg of the three phase MMC an be expressed as (13)

$$\dot{x}(t) = Ax(t) + \sum_{i=1}^{2}(B_{ix}u_i) + d(t) \quad (13)$$

where $x = [i_{v,j}, i_{diff,j}, v^{\Sigma}_{u,j}, v^{\Sigma}_{l,j}]^T$ is the state vector, $u = [u_1 u_2]^T = [n_{u,j} n_{l,j}]^T$ is the input vector, $d(t)$ is the disturbance and

$$A = \begin{bmatrix} -\frac{(R+2R_c)}{L+2L_c} & 0 & 0 & 0 \\ 0 & -\frac{R}{L} & 0 & 0 \\ 0 & 0 & 0 & 0 \\ 0 & 0 & 0 & 0 \end{bmatrix}$$

$$B_{ix} = \begin{bmatrix} B_1 x(t) & B_2 x(t) \end{bmatrix}$$

$$B_1 = \begin{bmatrix} 0 & 0 & \frac{1}{(L+2L_c)N} & 0 \\ 0 & 0 & \frac{-1}{2NL} & 0 \\ \frac{-1}{2C} & \frac{1}{C} & 0 & 0 \\ 0 & 0 & 0 & 0 \end{bmatrix}$$

$$B_2 = \begin{bmatrix} 0 & 0 & 0 & \frac{-1}{(L+2L_c)N} \\ 0 & 0 & 0 & \frac{-1}{2NL} \\ 0 & 0 & 0 & 0 \\ \frac{1}{2C} & \frac{1}{C} & 0 & 0 \end{bmatrix}$$

$$d(t) = \begin{bmatrix} \frac{2v_{f,j}(t)}{(L+2L_c)} \\ \frac{V_{dc}(t)}{2L} \\ 0 \\ 0 \end{bmatrix}$$

Equation (13) shows that the MMC is a bilinear system with multiple inputs and outputs.

III. Proposed Control Method for the MMC

In this work, the bisection algorithm is employed to reduce the search space for finding the optimum insertion index. The algorithm can be summarized as:

- Evaluate $n_{u,j} = 0, n_{l,j} = N$ and $n_{u,j} = N, n_{l,j} = 0$ *i.e.* the extreme on both ends
- if $n_{u,j} = 0, n_{l,j} = N$ gives lower cost then evaluate $n_{u,j} = N/4, n_{l,j} = N - n_{u,j}$ else evaluate $n_{u,j} = N - N/4, n_{l,j} = N - n_{u,j}$
- Then evaluate $n_{u,j} = N/4 + N/8, n_{l,j} = N - n_{u,j}$ and $n_{u,j} = N/4 - N/8, n_{l,j} = N - n_{u,j}$ else evaluate $n_{u,j} = N - N/4 - N/8, n_{l,j} = N - n_{u,j}$ and $n_{u,j} = N - N/4 + N/8, n_{l,j} = N - n_{u,j}$
- if from above $n_{u,j} = N/4 + N/8$ gives minimum cost then evaluate $n_{u,j} = N/4 + N/8 + N/16$ and $n_{u,j} = N/4 + N/8 - N/16$ with $n_{l,j} = N - n_{u,j}$
- Stop this procedure when $N/(2^k)$ is $<= 1$ for some k, where k is an integer
- Finally, once the insertion index that minimizes the cost function is found then apply reduced indirect FCS-MPC [6] with a maximum change of two in insertion index obtained from bisection algorithm. This is done only for the first time step within the prediction horizon. For the following time steps a maximum change of one is allowed in insertion index.

An illustrative example of the above procedure is shown in Fig. 2. The options in the highlighted area are the ones that give minimum cost at each step of above procedure. Among these options, the one that minimizes the cost function is forwarded to reduced indirect FCS-MPC. For example, if $N = 20$ then number of options evaluated will be $7 + 25 = 32$ for the first time step within the prediction horizon.

It is noted that in above $n_{u,j} = N/2$ is not evaluated on purpose as the algorithm will automatically converge to it if this is the optimal solution. This will happen because in the last step a maximum change of two is allowed in the insertion index. This approach significantly reduces the search space for reaching optimal insertion index without compromising on the performance. The proposed approach has similar dynamic performance as compared to full indirect FCS-MPC which will be demonstrated by simulations later. Moreover, this approach can easily be extended to MMCs with large number of SMs as compared to [13] without much increase in computational burden. For instance, for $N = 100$, the number of options to be evaluated for the proposed method in the first time step will be just $13 + 25 = 38$. However, if [13] has to include even one more option in the first time step for $N = 100$ then it has to evaluate 49 options in the first time step within the prediction horizon. The comparison of computational burden of different approaches for a prediction horizon (denoted by p) of three steps for an MMC with 20 SMs per arm is shown in Table-I.

TABLE I
NUMBER OF POSSIBLE CONTROL OPTIONS FOR DIFFERENT FCS-MPC STRATEGIES (P=3, 20 SMS/ARM)

Full Indirect FCS-MPC $(N+1)^{2p}$	**Reduced Indirect FCS-MPC** $(3)^{2p}$	**Modified Reduced Indirect FCS-MPC** $25 \cdot (3)^{2(p-1)}$	**Proposed Method** $32 \cdot (3)^{2(p-1)}$
85,766,121	729	2,025	2,592

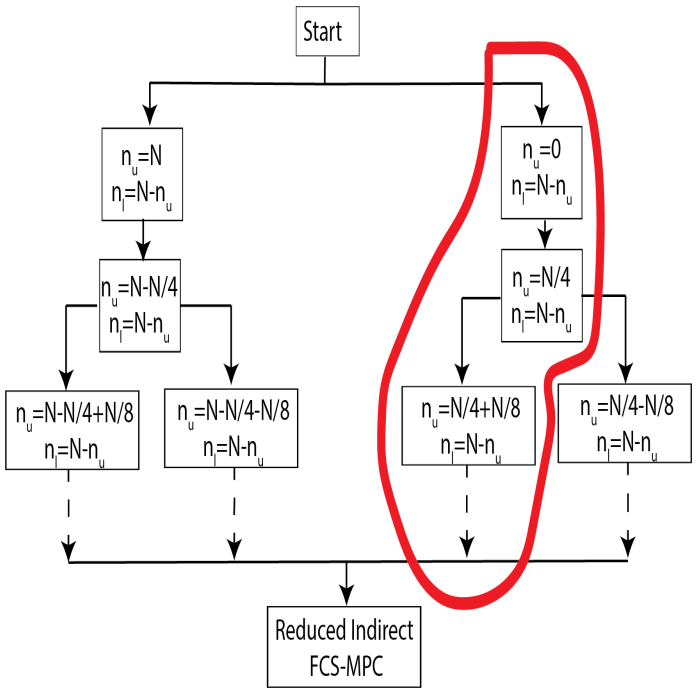

Fig. 2. Block diagram for Proposed Method

The cost function used for the proposed method is given as:

$$J_j = \lambda_1(i_{v,j,ref} - i_{v,j})^2 + \lambda_2(i_{diff,ref} - i_{diff,j})^2 + \lambda_3(2v_{dc,ref} - v^{\Sigma}_{u,j,avg} - v^{\Sigma}_{l,j,avg})(i_{diff,ref} - i_{diff,j}) + \lambda_4(v^{\Sigma}_{u,j,avg} - v^{\Sigma}_{l,j,avg})\Delta W \quad (14)$$

where the states are predicted by applying forward Euler approximation on (13). The λ's are the weighting factors for setting the relative importance between the control objectives. The first term in the cost function is used to keep the ac-side current at its reference, the second term is for minimizing the ac-components in the differential currents, the third term is to maintain the total leg voltage at $2V_{dc}$ and the fourth term is to regulate energy difference between the arms to zero. ΔW is the instantaneous energy difference between the lower and upper arm. The third and fourth term would only act if the average summation voltages of both arms is not equal to $2V_{dc}$ and the average difference voltages between both arms is not zero respectively. The average voltages are obtained through moving average filters. The third term would increase the differential current if the summation voltage is less than $2V_{dc}$ so that the SMs capacitors are charged more and vice versa in order to decrease the cost function. Similarly, the ΔW would act to reduce the arm energy difference of the two arms. The change in ΔW can be expressed as [15]:

$$\frac{dW_{\Delta}}{dt} = (v^{\Sigma}_{u,j} + v^{\Sigma}_{l,j})\frac{-i_{v,j}}{2} + (v^{\Sigma}_{u,j} - v^{\Sigma}_{l,j})i_{diff,j} \quad (15)$$

In the above expression, the sum of the voltages of both arms would be close to $2V_{dc}$ and it would be constant if the second harmonic component is ignored. $i_{v,j}$ is a fundamental frequency sinusoidal component. This implies that the first term in (15) is predominantly sinusoidal at the fundamental frequency. The second term *i.e.* based on the voltage difference of the two arms is sinusoidal at the fundamental frequency, while $i_{diff,j}$ would be close to a dc component. Thus, the second term would also be predominantly sinusoidal at the fundamental frequency. Now, unless these two terms in (15) cancel each other perfectly, the sum would be a predominantly sinusoidal signal, implying that also the integral *i.e.* W_{Δ} would be a sinusoidal signal. With this in mind, it is easy to see that the last term in the objective function becomes a sinusoidal term if $v^{\Sigma}_{u,j,avg} - v^{\Sigma}_{l,j,avg}$ is not equal to zero. This sinusoidal term is then indirectly compensated by the minimization converging to a situation with a corresponding (transient) sinusoidal term in the differential current.

It is important to highlight here that the cost function proposed in [6] cannot ensure the long term stability of summation voltages. As highlighted in [16], differential current reference adjustment is required by PI control over summation voltages or its equivalent within MPC implementation, in order to properly track the leg and arm voltages. Similarly, in the conventional cascaded energy based control [17], outer loop energy controllers are used to provide the references for different frequency components. This is because of the assumption of equal input and output power when determining the reference for differential current and this assumption will be violated by any microscopic losses and/or numerical inaccuracies. However, in the proposed cost function no such correction of differential current reference or use of outer loop is required. The third and fourth term included in (14) automatically induce the required change in differential current whenever the summation voltages are not at their reference.

The references for ac-side current, summation voltages and differential current are as in [13]. However, for the sake of completeness the reference selection is repeated here. The power equations in the dq frame are used to obtain the reference value for the ac-side current as follows:

$$i_d = \frac{2}{3}\frac{Pv_d + Qv_q}{v_d^2 + v_q^2} \quad (16a)$$

$$i_q = \frac{2}{3}\frac{Pv_q - Qv_d}{v_d^2 + v_q^2} \quad (16b)$$

Then by dq to abc transformation, the reference current can be obtained in the abc frame. The reference for the differential current is given as:

$$I_{dc,ref} = -\frac{P}{V_{dc,ref}}, I_{diff,ref} = \frac{I_{dc,ref}}{3} \quad (17)$$

The above reference, as highlighted before is based on the assumption of equal input and output power and is the main reason for proposing the new cost function (14). For SM capacitor voltage balancing task, the conventional sorting algorithm is used as in [13].

IV. Simulation Results

The block diagram for calculation of insertion indices by the proposed methodology is shown in Fig. 3. The performance of

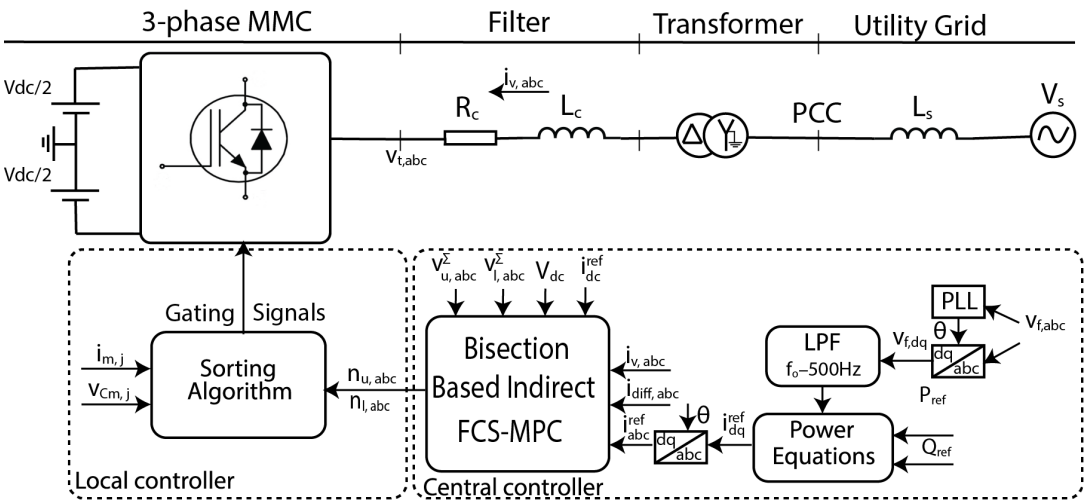

Fig. 3. Control Block Diagram of MMC

the proposed strategy is validated by performing simulations on a three-phase MMCs with 18 SMs per arm and compared with the full indirect FCS-MPC. The parameters used for simulation are summarized in Table-II. The scenario used for simulation is as follows. At $t = 0$ the reference values of active and reactive power are set to $25kW$ and $0KVar$, respectively and at $t = 0.12s$ a real power reversal command is applied by changing active power set point to $-25kW$.

TABLE II
SIMULATION PARAMETERS

Parameter	Value
MMC nominal power (base power)	60 kVA
AC system nominal voltage (base voltage)	400 V
Nominal frequency	50 Hz
Arm inductance (L)	1.5 mH
Arm resistance (R)	0.1Ω
Submodule capacitance (C)	20000μF
Transformer voltage rating (T)	400 V / 400 V
Transformer power rating	60 kVA
Transformer inductance	0.03 pu
Transformer resistance	0.01 pu
DC side reference voltage	700 V
Number of SMs per arm (N)	18
Sampling time (Ts)	70μs

The performance of all the state variables with the application of the proposed method under active power reversal command is depicted in Fig. 4. In Fig. 4(a) the changes in the active power are shown. In Fig. 4(b) the phase-a current is shown. It can be observed that the dynamic response is very good. The differential current performance of phase a is shown in Fig. 4(c) which shows that it tracks it's reference both in steady-state as well as in transient state. It can be observed that the differential current adjusts itself whenever the average of summation voltages is not at their reference. This action is happening due to the proposed cost function (14). The summation of capacitor voltages in the lower arm of phase a are depicted in Fig. 4(d). It can be seen that the average value of summation voltages is around their reference.

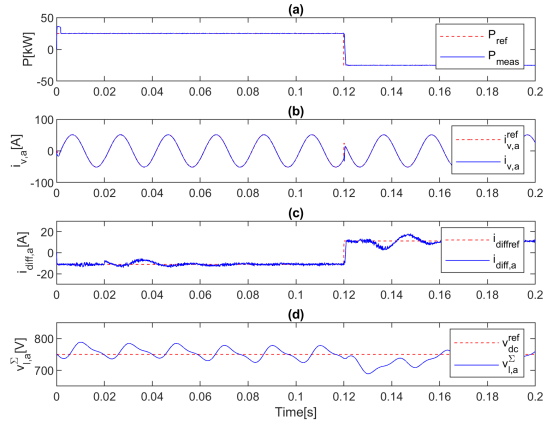

Fig. 4. Proposed Method: (a) active power, (b) phase-a current, (c) phase-a differential current, (d) summation of the capacitor voltages in the lower arm of phase a

Figure 5 shows the dynamic response of the d-axis component of ac-side current which validates that the proposed methodology has similar dynamic and steady state performance as full indirect FCS-MPC.

In Fig. 6, a comparison between the proposed cost function and the conventional cost function without the third and fourth term is shown. Figure 6(a,b) show the response of differential current and summation voltage in lower arm of phase a for the proposed cost function. It can be seen that the summation voltages return to their reference and differential current adjusts itself when summation voltages are not at their reference. Figure 6(c,d) show the response for conventional

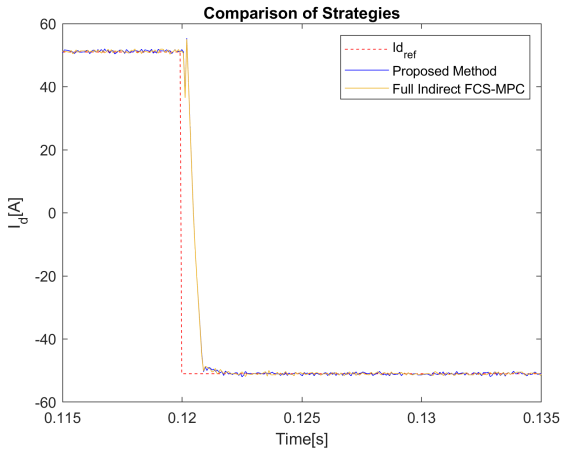

Fig. 5. Comparison of Results for d-axis component of ac-side current

cost function. It can be seen that differential current tracking becomes accurate. However, the summation voltages are not able to track their reference and slowly start to diverge away from their reference. This validates the importance of the proposed cost function.

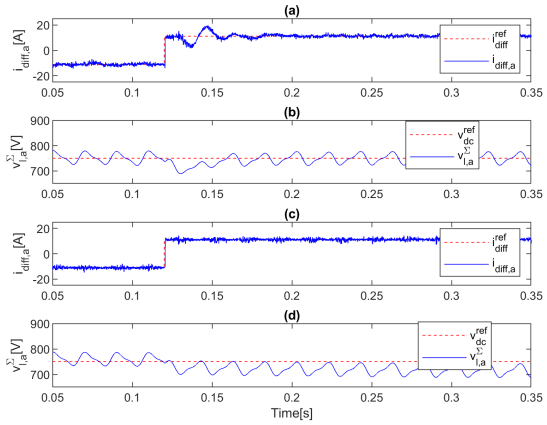

Fig. 6. Comparison of Results for Proposed and Conventional Cost Function

Finally, it was also noted, that the performance of the proposed approach is more close to full indirect FCS-MPC when the cost function is just quadratic as compared to (14). However, then as highlighted before additional control on differential current would be required for regulating the summation voltages in each arm.

V. Conclusion

In this paper, a bisection algorithm based indirect FCS-MPC method for MMCs has been presented. Moreover, a new cost function for indirect FCS-MPC is also proposed which eliminates the need for an outer loop or additional control on differential current to regulate the summation voltages in each arm. The proposed method gives similar steady state and dynamic performance as compared to full indirect FCS-MPC at a much lower computational burden. The proposed strategy can also be easily extended to MMCs with large number of SMs without much increase in computational burden in comparison to other indirect FCS-MPC strategies.

References

[1] K. Sharifabadi, L. Harnefors, H.-P. Nee, S. Norrga, and R. Teodorescu, *Design, Control and Application of Modular Multilevel Converters for HVDC Transmission Systems.* United States: Wiley-IEEE press, 2016.

[2] T. Geyer, Model Predictive Control of High Power Converters and Industrial Drives, Hoboken, NJ, USA:Wiley, 2016.

[3] A. Dekka, B. Wu, R. L. Fuentes, M. Perez and N. R. Zargari, "Evolution of Topologies, Modeling, Control Schemes, and Applications of Modular Multilevel Converters," *IEEE Journal of Emerging and Selected Topics in Power Electronics,* vol. 5, no. 4, pp. 1631-1656, Dec 2017

[4] A. Antonio-Ferreira, C. Collados-Rodriguez and O. Gomis-Bellmunt, "Modulation techniques applied to medium voltage modular multilevel converters for renewable energy integration: A review", *Electric Power Systems Research,* vol. 155, no. 7, pp. 21-39, Feb 2018

[5] A. Dekka, B. Wu, V. Yaramasu, R. L. Fuentes and N. R. Zargari, "Model Predictive Control of High-Power Modular Multilevel Converters—An Overview," *IEEE Journal of Emerging and Selected Topics in Power Electronics,* vol. 7, no. 1, pp. 168-183, March 2019

[6] M. Vatani, B. Bahrani, M. Saeedifard and M. Hovd, "Indirect Finite Control Set Model Predictive Control of Modular Multilevel Converters," *IEEE Transactions on Smart Grid,* vol. 6, no. 3, pp. 1520-1529, May 2015

[7] Z. Gong, P. Dai, X. Yuan, X. Wu and G. Guo, "Design and Experimental Evaluation of Fast Model Predictive Control for Modular Multilevel Converters," *IEEE Transactions on Industrial Electronics,* vol. 63, no. 6, pp. 3845-3856, June 2016

[8] B. Gutierrez and S. Kwak, "Modular Multilevel Converters (MMCs) Controlled by Model Predictive Control With Reduced Calculation Burden," *IEEE Transactions on Power Electronics,* vol. 33, no. 11, pp. 9176-9187, Nov. 2018

[9] M. H. Nguyen and S. Kwak, "Simplified Indirect Model Predictive Control Method for a Modular Multilevel Converter," *IEEE Access,* vol. 6, pp. 62405-62418, 2018

[10] J. Huang et al., "Priority Sorting Approach for Modular Multilevel Converter Based on Simplified Model Predictive Control," *IEEE Transactions on Industrial Electronics,* vol. 65, no. 6, pp. 4819-4830, June 2018

[11] P. Liu, Y. Wang, W. Cong and W. Lei, "Grouping-Sorting-Optimized Model Predictive Control for Modular Multilevel Converter With Reduced Computational Load," *IEEE Transactions on Power Electronics,* vol. 31, no. 3, pp. 1896-1907, March 2016

[12] A. Dekka, B. Wu, V. Yaramasu and N. R. Zargari, "Dual-Stage Model Predictive Control With Improved Harmonic Performance for Modular Multilevel Converter," *IEEE Transactions on Industrial Electronics,* vol. 63, no. 10, pp. 6010-6019, Oct. 2016

[13] S. Hamayoon, M. Hovd, J. A. Suul and M. Vatani, "Modified Reduced Indirect Finite Control Set Model Predictive Control of Modular Multilevel Converters," *IEEE COMPEL 2020*, Aalborg, Denmark, pp. 1-6,

[14] P. Cortes et al., "Guidelines for weighting factors design in Model Predictive Control of power converters and drives," *2009 IEEE International Conference on Industrial Technology*, 2009, pp. 1-7

[15] F. Zhang, W. Li and G. Joós, "A Voltage-Level-Based Model Predictive Control of Modular Multilevel Converter," *IEEE Transactions on Industrial Electronics*, vol. 63, no. 8, pp. 5301-5312, Aug. 2016

[16] X. Chen, J. Liu, S. Song, S. Ouyang, H. Wu and Y. Yang, "Modified Increased-Level Model Predictive Control Methods With Reduced Computation Load for Modular Multilevel Converter," *IEEE Transactions on Power Electronics*, vol. 34, no. 8, pp. 7310-7325, Aug. 2019

[17] A. Antonopoulos, L. Angquist and H. Nee, "On dynamics and voltage control of the Modular Multilevel Converter," *2009 13th European Conference on Power Electronics and Applications*, 2009, pp. 1-10.